

LEARNING A NONLINEAR DYNAMICAL SYSTEM MODEL OF GENE REGULATION: A PERTURBED STEADY-STATE APPROACH

BY ARWEN MEISTER, YE HENRY LI¹, BOKYUNG CHOI AND WING HUNG WONG²

Stanford University

Biological structure and function depend on complex regulatory interactions between many genes. A wealth of gene expression data is available from high-throughput genome-wide measurement technologies, but effective gene regulatory network inference methods are still needed. Model-based methods founded on quantitative descriptions of gene regulation are among the most promising, but many such methods rely on simple, local models or on ad hoc inference approaches lacking experimental interpretability. We propose an experimental design and develop an associated statistical method for inferring a gene network by learning a standard quantitative, interpretable, predictive, biophysics-based ordinary differential equation model of gene regulation. We fit the model parameters using gene expression measurements from perturbed steady-states of the system, like those following overexpression or knockdown experiments. Although the original model is nonlinear, our design allows us to transform it into a convex optimization problem by restricting attention to steady-states and using the lasso for parameter selection. Here, we describe the model and inference algorithm and apply them to a synthetic six-gene system, demonstrating that the model is detailed and flexible enough to account for activation and repression as well as synergistic and self-regulation, and the algorithm can efficiently and accurately recover the parameters used to generate the data.

Introduction. Complex interactions between many genes give rise to the biological structure and function that sustain life. The Central Dogma [Crick (1970), Jacob and Monod (1961)] provides a qualitative description of how these processes occur, but precise quantitative modeling is still needed [Rosenfeld (2011), Tyson, Chen and Novak (2003)]. Research into the detailed mechanisms of gene expression over the past few decades has shown that expression is regulated by a complex system of gene interactions. Recently, microarray and sequencing technologies [DeRisi, Iyer and Brown (1997), Mortazavi et al. (2008), Ren et al. (2000), Robertson et al. (2007)] have enabled high-throughput genome-wide expression level measurements. This data enables detailed study of gene networks

Received July 2012; revised March 2013.

¹Supported in part by NIH Grant GM007276.

²Supported in part by NIH Grant R01-HG006018 and NSF Grant DMS-09-06044.

Key words and phrases. Gene expression regulation, thermodynamic model, gene network inference, constrained convex optimization, parameter selection, perturbed steady-state, genome-wide expression measurements, synthetic gene network.

[Bar-Joseph et al. (2003), Holstege et al. (1998), Hu, Killion and Iyer (2007), Lee et al. (2002), Segal et al. (2003), Tegner et al. (2003), Zhou et al. (2007)]. The goal is to understand how genes interact to give rise to the biochemical complexity that allows organisms to live, grow and reproduce.

Gene expression measurements contain information useful for reconstructing the underlying interaction structure [DeRisi, Iyer and Brown (1997), Holstege et al. (1998), Hughes et al. (2000)] because gene regulatory systems have a defined ordering [Avery and Wasserman (1992)], forming pathways that connect to form networks [Alon (2007), De Smet and Marchal (2010)]. Many gene regulation pathways have been discovered over the past few decades [Alberts et al. (2007), Hartwell et al. (2010)]. At the turn of the century, researchers began applying statistical tools to genome-wide expression data to understand complex gene interactions. Eisen et al. showed that genes from the same pathways and with similar functions cluster together by expression pattern [Eisen et al. (1998)]. Soon afterward, module-based network inference methods appeared, which group co-expressed genes into cellular function modules [Bar-Joseph et al. (2003), Segal et al. (2003)]. Recently, methods based on descriptive but nonmechanistic mathematical models [Bansal et al. (2007), Faith et al. (2007), Friedman (2004), Gardner et al. (2003), Tegner et al. (2003)] have gained prominence. These models describe gene regulation quantitatively and can be used to simulate and predict systems behaviors [Dehmer et al. (2011), Palsson (2011)]. However, more work is needed to develop effective model-based methods for inferring gene network structure from experimental data.

Existing inference methods typically rely either on heuristic approaches or on very simple, local models, like linear differential equation models in a neighborhood of a particular steady-state. Statistical correlation is a common method of establishing network connections [Dehmer et al. (2011)] and can be very useful when hundreds or thousands of genes are monitored under specific, local cellular conditions (e.g., for grouping genes with similar functions). However, this approach works poorly when perturbations drive the network far from the original steady-state. Global nonlinear models are essential to account for complex global system behaviors, like the transformation of a normal cell into a cancerous cell due to the amplification of a particular gene.

As a basis for our inference approach, we chose a standard global nonlinear model: the quantitative, experimentally interpretable biophysics-based ordinary differential equation (ODE) gene regulation model of Bintu et al. (2005b, 2005a). Many models of this type have been proposed, and the idea traces back to the beginning of systems biology in the biophysics field [Ackers, Johnson and Shea (1982), Shea and Ackers (1985), von Hippel et al. (1974)], but the Bintu model is widely accepted within the biophysics community [Bintu et al. (2005b)]. The Bintu model is based on the thermodynamics of RNA transcription, the process at the core of gene expression regulation [Holstege et al. (1998), Hu, Killion and Iyer (2007)]. Transcription occurs when RNA polymerase (RNAP) binds the gene promoter; transcription factors (TFs) can modulate the RNAP binding energy to acti-

vate or repress transcription. RNA transcripts are then translated into protein. Bintu models the mechanism of transcription in detail, using physically interpretable parameters. The form of the equations is rich and flexible enough to include the full range of gene regulatory behavior. Another notable biophysics-based model is that of the annual DREAM competition, but it has many biochemical assumptions and model parameters, like the Hill coefficient of transcription factor binding events, that cannot be estimated using gene expression measurements, so the network reconstruction requires ad hoc inference methods to learn the underlying gene interactions [Marbach et al. (2010), Pinna, Soranzo and de la Fuente (2010), Schaffter, Marbach and Floreano (2011), Yip et al. (2010)]. Compared to the DREAM model, the Bintu model has the advantages of simplicity and interpretability, and better lends itself to principled inference.

In this paper, we propose an experimental design and associated statistical method for inferring an unknown gene network by fitting the ODE-based Bintu gene regulation model. The required data is gene expression measurements at a set of perturbed steady-states induced by gene knockdown and overexpression [Huang et al. (2005)]. We show how to design a sequence of experiments to collect the data and how to use it to fit the parameters of the Bintu model, leading to a set of ODEs that quantitatively characterize the regulatory network. Although the original fitting problem is nonlinear, we can transform it into a convex optimization problem by restricting our attention to steady-states. We use the lasso [Tibshirani (1996)] for parameter selection. As a proof of principle, we test the method on a simulated embryonic stem cell (ESC) transcription network [Chickarmane and Peterson (2008)] given by a system of ODEs based on the Bintu model. Here, we demonstrate that the inference algorithm is computationally efficient, accounts for synergistic regulation and self-regulation, and correctly recovers the parameters used to generate the data. Furthermore, the method requires only a set of steady-state gene expression measurements. Experimental researchers in the biological sciences can use this method to infer gene networks in a much more principled, detailed manner than earlier approaches allowed.

Dynamical systems model. We model gene expression regulation as a dynamical system. Let $x \in \mathbb{R}^n$ represent RNA concentrations and $y \in \mathbb{R}^n$ represent protein concentrations corresponding to a set of n genes. We assume that the production rate of the RNA transcript x_i of gene i is proportional to the probability $f(y)$ that RNA polymerase (RNAP) is bound to the promoter. That is, we assume that RNA transcription occurs at a rate τ_i whenever RNAP is bound to the promoter. We model the probability that RNAP is bound to the promoter as a nonlinear function f of y , since RNAP binding is regulated by a set of TFs. Further, we assume that the production rate of protein product y_i of gene i is proportional to the concentration of the RNA transcript x_i , and that both the RNA transcript and

protein products of gene i degrade at fixed rates (λ_i^{RNA} , $\lambda_i^{\text{Protein}}$),

$$(1) \quad \begin{aligned} \frac{dx_i}{dt} &= \tau_i f_i(y) - \lambda_i^{\text{RNA}} x_i, \\ \frac{dy_i}{dt} &= r_i x_i - \lambda_i^{\text{Protein}} y_i. \end{aligned}$$

Based on the thermodynamics of RNAP and TF binding, one can deduce the following form for f_i [Bintu et al. (2005b, 2005a)]:

$$(2) \quad f_i(y) = \frac{b_{i0} + \sum_{j=1}^m b_{ij} \prod_{k \in S_{ij}} y_k}{1 + \sum_{j=1}^m c_{ij} \prod_{k \in S_{ij}} y_k},$$

where S_{ij} lists the gene products that interact to form a regulatory complex, and b_{ij} , c_{ij} are nonnegative coefficients that must satisfy $c_{ij} \geq b_{ij} \geq 0$. (We assume that the concentration of each complex is proportional to the product of the concentrations of the constituent proteins, and absorb the proportionality constant into corresponding coefficients b_{ij} , c_{ij} .) The coefficients b_{ij} and c_{ij} depend on the binding energies of regulator complexes to the promoter. b_{i0} and c_{i0} correspond to the case when the promoter is not bound by any regulator ($\prod_{k \in S_{i0}} y_k = 1$), and the coefficients are normalized so that $c_{i0} = 1$. Details and a derivation are given in the [Appendix](#).

The form of f_i allows us to model the full spectrum of regulatory behavior in quantitative detail. Terms that appear in the denominator only are repressors, and the degree of repression depends on the magnitude of the coefficient, while terms that appear in the numerator and denominator may act as either activators or repressors depending on the relative magnitudes of the coefficients and the current gene expression levels. Terms may represent either single genes or gene complexes. The model can even be extended to account for environmental factors that affect gene regulation, though we will not discuss it further here.

As an example, consider the simple two-gene network shown in Figure 1. Suppose that genes 1 and 2 have RNA concentrations x_1 , x_2 , and protein concentrations y_1 , y_2 , respectively, and that gene 1 is activated by protein 2 and repressed

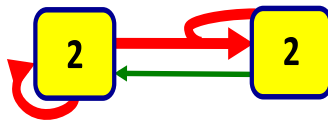


FIG. 1. Simple two-gene network example described by equation (3) (with parameters $b_{11} = c_{11} = 0.1$ for activators; $c_{12} = 10$ for repressors; and $b_{10} = 0.01$ for constants in the numerator). Gene 1 is activated by the protein product of gene 2 and repressed by its own product (an example of self-regulation). Gene 2 is repressed by a complex formed by the product of gene 1 and its own product (synergistic self-regulation). In the diagram, the edge colors indicate activation (green) or repression (red) and the edge weights indicate coefficient sizes, illustrated above with typical sizes.

by its own product (protein 1), while gene 2 is repressed by a complex formed by proteins 1 and 2. The situation corresponds to the following equations:

$$(3) \quad \begin{aligned} \frac{dx_1}{dt} &= \tau_1 \frac{b_{10} + b_{11}y_2}{1 + c_{11}y_2 + c_{12}y_1} - \lambda_1^{\text{RNA}}x_1, & \frac{dy_1}{dt} &= r_1x_1 - \lambda_1^{\text{Protein}}y_1, \\ \frac{dx_2}{dt} &= \tau_2 \frac{b_{20}}{1 + c_{21}y_1y_2} - \lambda_2^{\text{RNA}}x_2, & \frac{dy_2}{dt} &= r_2x_2 - \lambda_2^{\text{Protein}}y_2. \end{aligned}$$

In the notation above, we have $S_{11} = \{2\}$, $S_{12} = \{1\}$, $S_{21} = \{1, 2\}$. The parameters $b_{10}, b_{11}, c_{11}, \dots$ determine the magnitude of the repression or activation. As this example shows, the model is flexible enough to capture a wide range of effects, including self-regulation (i.e., regulation of a gene by its own protein product, most commonly as repression) and synergistic regulation by protein complexes (two or more proteins bound together to form a regulatory unit), in quantitative detail. Furthermore, the model is predictive: if we know or can infer the coefficients in the model, we can predict the future behavior of the system starting from any initial condition.

Inference problem. The model given by equations (1) and (2) fully describes the evolution of RNA and protein levels and provides a comprehensive, quantitative model of gene regulation, provided we know the parameters. Unfortunately, b_{ij}, c_{ij} are extremely difficult to measure, as they depend on binding energies of RNAP and TFs to the gene promoter. The sheer number of measurements required to characterize all possible TFs (both individual proteins and complexes) also makes this approach infeasible. Therefore, our goal is to use a systems level approach to fit the model using RNA expression data. Specifically, we will assume that $\tau_i, \lambda_i^{\text{RNA}}, \lambda_i^{\text{Protein}}$ are known or can be measured (if these quantities are not available, we can simply absorb them into the coefficients b_{ij}, c_{ij} , although more accurate rate estimates will likely improve the coefficient estimates). Our data will be measurements of the RNA concentrations x at many different cellular steady-states (which correspond to steady-states of the dynamical system). The problem is to infer the values of the coefficients b_{ij}, c_{ij} .

Linear problem at steady-state. The key to solving this problem efficiently is to restrict our attention to steady-states, as proposed by Choi (2012). This restriction allows us to transform a nonlinear ODE fitting problem into a linear regression problem. A steady-state of the system is one in which RNA and protein levels are constant: $\frac{dx_i}{dt} = \frac{dy_i}{dt} = 0$. Steady-states of the system correspond to cell states with roughly constant gene expression levels, like embryonic stem cell, skin cell or liver cell. In contrast, an embryonic stem cell in the process of differentiating is not in steady-state. Perturbed steady-states are particularly interesting. After a perturbation like gene knockdown, a cell's gene expression levels are in flux for some time

while they adjust to the change. Eventually, if it is still viable, the cell may settle to a new steady-state [Huang et al. (2005)]. These perturbed steady-states are especially helpful for understanding gene regulation.

In our model, the steady-state conditions $\frac{dx_i}{dt} = \frac{dy_i}{dt} = 0$ mean that

$$0 = \tau_i f_i(y) - \lambda_i^{\text{RNA}} x_i, \quad 0 = r_i x_i - \lambda_i^{\text{Protein}} y_i \implies y_i = \frac{r_i x_i}{\lambda_i^{\text{Protein}}}.$$

Defining $\tilde{f}_i(z) = f_i\left(\frac{r_i}{\lambda_i^{\text{Protein}}} z\right)$ yields

$$0 = \tau_i \tilde{f}_i(x) - \lambda_i^{\text{RNA}} x_i.$$

Absorbing the constants into the coefficients b_{ij}, c_{ij} (so that $\tilde{b}_{ij} = b_{ij} \prod_{k \in S_{ij}} \frac{r_k}{\lambda_k^{\text{Protein}}}$, $\tilde{c}_{ij} = c_{ij} \prod_{k \in S_{ij}} \frac{r_k}{\lambda_k^{\text{Protein}}}$), we obtain the final equation

$$\tau_i \frac{b_{i0} + \sum_j b_{ij} \prod_{k \in S_{ij}} x_k}{1 + \sum_j c_{ij} \prod_{k \in S_{ij}} x_k} - \gamma_i x_i = 0$$

or

$$\tau_i \left(b_{i0} + \sum_j b_{ij} \prod_{k \in S_{ij}} x_k \right) - \gamma_i x_i \left(1 + \sum_j c_{ij} \prod_{k \in S_{ij}} x_k \right) = 0$$

(by multiplying both sides by the denominator). The last equation is linear in the coefficients b_{ij}, c_{ij} ! In order to solve for b_{ij}, c_{ij} , we will need to collect many different expression measurements x at both naturally occurring and perturbed steady-states. Each steady-state measurement will lead to a different linear equation. These equations can be arranged into a linear system that we can solve for the coefficients.

Problem formulation. Our problem is to find b_{ij}, c_{ij} such that

$$\begin{aligned} 0 = \tau_i \left(b_{i0} + \sum_j b_{ij} \prod_{k \in S_{ij}} x_k^{(m)} \right) \\ - \gamma_i x_i \left(1 + \sum_j c_{ij} \prod_{k \in S_{ij}} x_k^{(m)} \right) \quad \forall m = 1, \dots, M, \end{aligned}$$

given RNA expression data $x^{(m)}$ at many different steady-state points $m = 1, \dots, M$ and known translation and degradation rates $\tau_i, \lambda_i^{\text{RNA}}, \lambda_i^{\text{Protein}}$. (The experimental means of collecting the necessary steady-state expression data will be discussed in the next section.) We solve a separate problem for each gene i , since the coefficients b_{ij}, c_{ij} in the differential equation $dx_i/dt = \dots$ for gene i are independent of the coefficients in the differential equations for other genes. Since

we cannot know ahead of time which potential regulatory terms $\prod_{k \in S_{ij}} x_k$ are actually involved, we include all possible terms up to second-order and look for sparse b_{ij}, c_{ij} , interpreting $c_{ij} = 0$ to mean that term $\prod_{k \in S_{ij}} x_k$ is not a regulator of gene i .

Consider gene 2 in the two-gene example. Suppose we have expression measurements for a naturally occurring steady-state (x_1^0, x_2^0) , and a perturbed steady-state following gene 1-knockout $(0, x_2^1)$. We obtain two linear equations in the coefficients b_{20}, c_{21} :

$$\begin{aligned} \tau b_{20} - \lambda_2 x_2^0 (1 + c_{21} x_1^0 x_2^0) &= 0 && \text{(steady-state } (x_1^0, x_2^0)), \\ \tau b_{20} - \lambda_2 x_2^1 &= 0 && \text{(steady-state } (0, x_2^1)). \end{aligned}$$

If we knew a priori that complex $x_1 x_2$ was the only regulator of gene 2, these two equations would allow us to solve for the coefficients ($b_{20} = \frac{\lambda_2 x_2^1}{\tau}$, $c_{21} = \frac{x_2^0 - x_2^1}{(x_2^0)^2}$). Typically we do not know the regulators beforehand, however, and we need to use the data to identify them. That is, we include all possible terms (up to second-order) in the equations:

$$\begin{aligned} \tau (b_{20} + b_{21} x_1^{(m)} x_2^{(m)} + b_{22} x_1^{(m)} + b_{23} x_2^{(m)}) \\ - \lambda_2 x_2^{(m)} (1 + c_{21} x_1^{(m)} x_2^{(m)} + c_{22} x_1^{(m)} + c_{23} x_2^{(m)}) \\ = 0 \end{aligned}$$

and estimate sparse coefficients b_{ij}, c_{ij} using several steady-state measurements $(x_1^{(m)}, x_2^{(m)})$. (We should find that the recovered coefficients $b_{21}, b_{22}, b_{23}, c_{22}, c_{23}$ are very close to zero, since the corresponding terms do not appear in the true equation.)

Temporarily suppressing the superscript m denoting the observation, we can compactly express the general system above by defining z_i as the vector with entries $z_i(j) = \prod_{k \in S_{ij}} x_k$ [with the convention that $z_i(0) = 1$, $z_i(j) = x_j$ for $j = 1, \dots, n$], which yields

$$0 = \tau_i b_i^T z_i - \gamma_i z_i(i) c_i^T z_i$$

for each observation ($m = 1, \dots, M$). If we form a matrix G_i by concatenating the row vectors $z_i^{(1)}, \dots, z_i^{(M)}$ and let D_i be a diagonal matrix with entries $z_i^{(m)}(i)$, $m = 1, \dots, M$, we can express this as

$$[\tau_i G_i \quad -\gamma_i D_i G_i] \begin{bmatrix} b_i \\ c_i \end{bmatrix} = 0$$

with the constraints $0 \leq b_i \leq c_i$, $c_i(0) = 1$. Stating the problem in this form elucidates the required number of steady-state measurements, M . If the linear system above were dense and had no constraints on the coefficients b_{ij}, c_{ij} , and the steady-state expression vectors were (numerically) linearly independent, then we would require $M = 2T_{n,k}$, where $T_{n,k}$ is the number of the terms in the rational-form

polynomial of degree k in n genes ($k = 2$ if we include up to second-order regulatory interactions). $T_{n,k}$ is equal to the number of subsets of $\{1, 2, \dots, n\}$ with k or fewer elements since each term represents an interaction between j distinct genes ($0 \leq j \leq k$), hence, $T_{n,k} = \sum_{j=0}^k \binom{n}{j} \leq n^k$ for $k \leq n$ ($T_{n,2} \leq n^2$, e.g.). However, the constraints reduce the dimension of the solution space [$c_i(0) = 1$ reduces it by 1, while $0 \leq b_i \leq c_i$ reduces it by up to n], and our algorithm also uses ℓ_1 -regression to search for sparse solutions, which may allow us to reconstruct the coefficients from far fewer measurements than $2T_{n,k}$.

Experimental approach. The set of steady-state gene expression measurements needed to fit the model can be generated via a systematic sequence of gene perturbation experiments. Figure 2 summarizes the overall approach to finding the regulatory interactions among a set of genes comprising a (roughly) self-contained

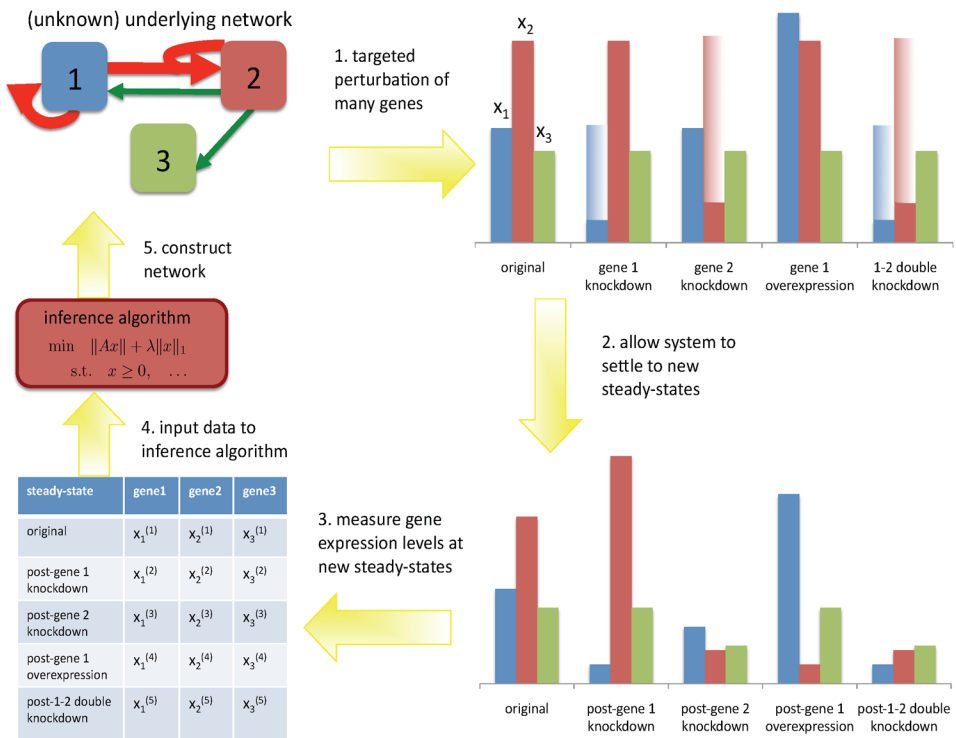


FIG. 2. *Experimental approach for gene network inference.* (1) *Design and perform perturbation experiments targeting each gene (or possibly pair of genes) in the network: these may include overexpression, knockdowns or knockouts.* (2) *Following each perturbation, allow the system to settle to a new steady-state.* (3) *Measure expression levels of all genes at each induced steady-state, and collect results in a data matrix.* (4) *Use steady-state expression data as input to inference algorithm.* (5) *Construct regulatory network from inference algorithm output.*

network of interest. First, molecular perturbations targeting each gene, or possibly pair of genes, in the network would be designed and applied one at a time. Following each perturbation, the cells would be allowed to settle down to a new steady-state, at which point the gene expression levels would be measured. The collection of gene expression measurements from different steady-states would be input to the inference algorithm described in the next section, which outputs a dynamical systems model of the gene network capable of predicting the behavior of the network following other perturbations. Perturbation data not used in the inference algorithm could be used to validate the recovered model.

The key experimental steps in this procedure, gene perturbations and gene expression measurements, are established technologies. Gene perturbations, including overexpression, knockdown and knockout, are routinely used in biological studies to investigate gene function. These experiments can be performed for many laboratory organisms and cell lines both *in vitro* and *in vivo* [Alberts et al. (2007)]. Overexpression experiments amplify a gene's expression level, usually by introducing an extra copy of the gene. Knockdown experiments typically use RNAi technology: the cell is transfected with a short DNA sequence, driven by a (possibly inducible) promoter element, that produces siRNA or shRNA that specifically binds the RNA transcripts of the gene of interest and triggers degradation. Morpholinos can also be used for gene knockdown. Gene knockout can be achieved by removing all or part of a gene to permanently disrupt transcription [Alberts et al. (2007)]. Overexpression [Rodriguez et al. (2007)], knockdown [Foygel et al. (2008), Rodriguez et al. (2007)] and knockout [Lengner et al. (2011)] experiments have all been performed for the Oct4 gene, which helps maintain the stem cell steady-state. In some cases, much of the work is already done: for example, the *Saccharomyces* Genome Deletion Project has a nearly complete library of deletion mutants [Winzeler (1999)].

Techniques for gene expression measurement are also well-established. Gene expression is usually measured at the transcript level: the RNA transcripts are extracted and reverse-transcribed into cDNA, which can be quantified with either RT-qPCR, microarray or sequencing technologies [Alberts et al. (2007), Mortazavi et al. (2008)]. Housekeeping gene expression measurements are used as controls to determine the expression levels of the genes of interest. The gene perturbations and subsequent expression measurements required to collect data for our inference algorithm may be time-consuming due to the large number of perturbations, but all the experimental techniques are quite standard and resources like deletion libraries can be extremely helpful.

Algorithm. We need to solve the linear system

$$[\tau_i G_i \quad -\gamma_i D_i G_i] \begin{bmatrix} b_i \\ c_i \end{bmatrix} = 0$$

for b_i, c_i , subject to the constraints $0 \leq b_i \leq c_i$, $c_i(0) = 1$. To account for measurement noise and encourage sparsity in b_i, c_i (since we know that each gene has only a few regulators), we will minimize the ℓ_2 -norm error with ℓ_1 regularization [Tibshirani (1996)], which leads to the convex optimization problem

$$(4) \quad \begin{aligned} & \text{minimize} \quad \left\| \begin{bmatrix} \tau_i G_i & -\gamma_i D_i G_i \end{bmatrix} \begin{bmatrix} b_i \\ c_i \end{bmatrix} \right\|_2 + \lambda (\|b_i\|_1 + \|c_i\|_1) \\ & \text{subject to} \quad 0 \leq b_i \leq c_i, \quad c_i(0) = 1, \end{aligned}$$

where λ is a parameter controlling sparsity that we can choose using cross-validation. Since the problem is convex, it can be solved very efficiently even for large values of n and m .

Nonidentifiability. Our model's ability to capture self-regulation is very powerful, but it also leads to a particular form of nonidentifiability. For certain forms of the equation, given only steady-state measurements, it can be impossible to determine whether self-regulation is either completely absent or present in every term. Specifically, any valid equation of the form

$$(5) \quad \frac{dx_i}{dt} = \frac{b_{i0} + \sum_{j=1}^N b_{ij} \prod_{k \in S_{ij}} x_k}{1 + \sum_{j=1}^N c_{ij} \prod_{k \in S_{ij}} x_k} - \gamma_i x_i, \quad b_{i0} < 1,$$

is indistinguishable at steady-state from any member of the following family of valid equations indexed by the constant w :

$$(6) \quad \frac{dx_i}{dt} = \frac{(wb_{i0} + \gamma_i)x_i + \sum_{j=1}^N wb_{ij} \prod_{k \in S_{ij}} x_i x_k}{1 + wx_i + \sum_{j=1}^N wc_{ij} \prod_{k \in S_{ij}} x_i x_k} - \gamma_i x_i, \quad w \geq \frac{\gamma}{1 - b_{i0}}.$$

We will refer to these as the “simple” and “higher-order” forms of the equation, respectively. The short proof of their equivalence is given in section S1 of the supplementary article [Meister et al. (2013)]. The condition $w \geq \frac{\gamma}{1 - b_{i0}}$ guarantees that $w > 0$ and $0 \leq wb_{i0} + \gamma_i \leq w$ (since $0 \leq b_{i0} < 1$) and $0 \leq wb_{ij} \leq wc_{ij}$ (since $0 \leq b_{ij} \leq c_{ij}$).

We can distinguish between these two alternative forms by measuring the derivative of the concentration away from steady-state and comparing it to the derivative predicted by each form of the equation. This requires only a few extra thoughtfully-selected measurements. The details are in section S2 of the supplement.

Simulated six-gene subnetwork in mouse ESC. To demonstrate the inference approach, we apply our method to a synthetic six-gene system based on the Oct4, Sox2, Nanog, Cdx2, Gcnf, Gata6 subnetwork in a mouse embryonic stem

cell (ESC). Chickarmane and Peterson (2008) developed this system based on a synthesis of knowledge about ESC gene regulation accumulated over the past two decades [Chickarmane and Peterson (2008)]. The network structure is shown in Figure 4(a), and the detailed model is given by the following system of ODEs in the six genes:

$$\begin{aligned}
 \frac{d[O]}{dt} &= (0.001 + [A] + 0.005[O][S] + 0.025[O][S][N]) \\
 &\quad / (1 + [A] + 0.001[O] + 0.005[O][S] \\
 &\quad \quad + 0.025[O][S][N] + 10[O][C] + 10[Gc]) \\
 &\quad - 0.1[O], \\
 \frac{d[S]}{dt} &= \frac{0.001 + 0.005[O][S] + 0.025[O][S][N]}{1 + 0.001[O] + 0.005[O][S] + 0.025[O][S][N]} \\
 &\quad - 0.1[S], \\
 \frac{d[N]}{dt} &= \frac{0.001 + 0.1[O][S] + 0.1[O][S][N]}{1 + 0.001[O] + 0.1[O][S] + 0.1[O][S][N] + 10[O][G]} \\
 &\quad - 0.1[N], \\
 \frac{d[C]}{dt} &= \frac{0.001 + 2[C]}{1 + 2[C] + 5[O][C]} - 0.1[C], \\
 \frac{d[Gc]}{dt} &= \frac{0.001 + 0.1[C] + 0.1[G]}{1 + 0.1[C] + 0.1[G]} - 0.1[Gc], \\
 \frac{d[G]}{dt} &= \frac{0.1 + [O] + 0.00025[G]}{1 + [O] + 0.00025[G] + 15[N]} - 0.1[G].
 \end{aligned}
 \tag{7}$$

This model has many of the same qualitative characteristics as the biological mouse ESC network [Chickarmane and Peterson (2008)]. In particular, the system can support four different steady-states: embryonic stem cell (ESC), differentiated stem cell (DSC), endoderm and trophectoderm, and can switch from one to another when certain genes' expression levels are changed. In the Oct4 equation, A represents an external activating factor whose concentration $[A]$ depends on the culture condition. Each of the four steady-states has a corresponding value of $[A]$: 10 for ESC and DSC, 25 for endoderm, and 1 for trophectoderm. For the remainder of this paper, we will regard $[A]$ as known. The explicit system of ODEs (7) allows us to generate data to fit our model and also to quantitatively compare our recovered solution to the ground truth. The qualitative similarity of this synthetic network to a real biological network gives us confidence that our results in this numerical experiment are likely to translate well to real biological networks.

We observe that the $Cdx2$, $Gcnf$ and $Gata6$ equations have alternative forms (provided we ignore the very small constant term in the $\frac{d[C]}{dt}$ equation and $[G]$

term in the $\frac{d[G]}{dt}$). With the minimum possible value of w , the alternative forms are as follows:

$$\begin{aligned}
 \frac{d[C]}{dt} &= \frac{0.95}{1 + 2.5[O]} & (w = 2), \\
 \frac{d[Gc]}{dt} &= \frac{0.1001[Gc] + 0.01[C][Gc] + 0.01[Gc][G]}{1 + 0.1[Gc] + 0.01[C][Gc] + 0.01[Gc][G]} \\
 &\quad - 0.1[Gc] & (w = 0.1), \\
 \frac{d[G]}{dt} &= \frac{0.111[G] + 0.111[O][G]}{1 + 0.111[G] + 0.111[O][G] + 1.67[N][G]} \\
 &\quad - 0.1[G] & (w = 0.111).
 \end{aligned}
 \tag{8}$$

To resolve the specific form, we will apply our method twice, once allowing self-regulation and again disallowing it. Then we will compare the two recovered forms of each equation and the quality of the fits to determine whether nonidentifiability exists in each case. If so, we will break the tie by examining derivatives.

To fit the model, we collect data on the expression levels of all six genes at many different steady-states. First we measure the expression levels at all four wildtype steady-states: SC, DSC, endoderm and trophectoderm. We also induce additional perturbed steady-states by simulating knockdowns and overexpression of each gene, based on physical gene perturbation experiments [Rodriguez et al. (2007), Zafarana et al. (2009)]. For a knockdown, we hold a gene at one-fifth of its steady-state expression level; for overexpression we hold a gene at twice its steady-state level. In each case we wait for the system to settle to a new steady-state, then measure the expression levels. Figure 3 shows the expression trajectories during Oct4 knockdown from the ESC steady-state as an example.

The details of the simulation are given in section S3 of the supplement. We begin by testing the algorithm on noiseless data. We solve the optimization problem (4) once, then we solve it again with additional constraints prohibiting self-regulation. In each case we use cross-validation to select the sparsity parameter λ (Figure S1). The quality of the fit is comparable for the latter three equations whether we restrict self-regulation or not, while for the first three equations restricting self-regulation has a significant negative impact on the fit (Table S1), indicating that the first three equations are unambiguous while the last three have two possible forms. To resolve the nonidentifiability in the latter three equations, we measure the derivatives of Cdx3, Gcnf and Gata6 immediately after some additional informative perturbations: Oct4, Cdx2 and Nanog knockouts, respectively (Figure S2). The test reveals that Gcnf and Gata6 have the simple form, while Cdx2 has a higher-order form. In this example, the original coefficients are recov-

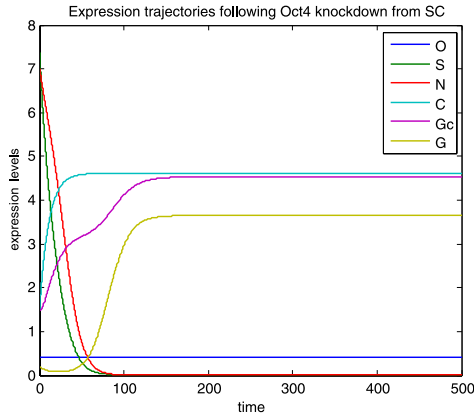


FIG. 3. Gene expression trajectories during an Oct4 knockdown from SC steady-state. The expression of Oct4 is artificially reduced to 20% of its SC steady-state expression level and held there, causing the expression levels of the targets of Oct4 to change in response, which in turn impact their targets. The system eventually reaches a new steady-state different from SC. We measure the vector of expression levels at the new steady-state and use it as data in the inference algorithm. Since Oct4 is knocked down, this induced steady-state does not provide useful information about the Oct4 equation, but it is useful for understanding the role of Oct4 and other genes in the equations of the remaining five genes.

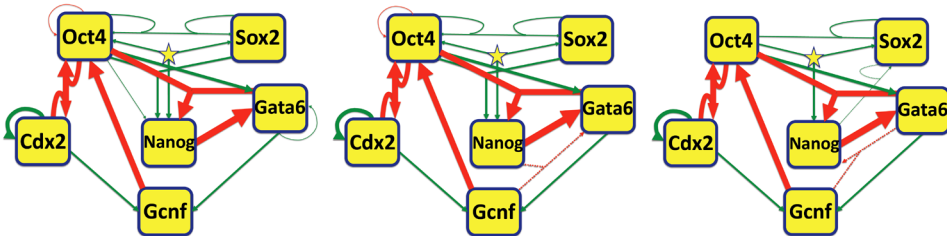


FIG. 4. Recovery of a synthetic gene regulatory network based on the biological ESC network using our inference algorithm. The diagrams represent systems of ODEs that quantitatively model the gene interactions. Edge color indicates activation (green) or repression (red), and edge weights correspond to coefficient magnitudes. The arrows point from regulator to target, and self-loops indicate self-regulation. The yellow star represents the third-order complex OSN. (In addition to all possible first- and second-order terms, we allow this special third-order term with a free coefficient.) The left figure represents the original system of ODEs used to generate the data. The center figure shows the network recovered using our inference algorithm on noiseless data, and the right figure shows the recovery with 1% noise added. Both recovered networks reflect coefficient thresholding at 0.1% (noiseless case) or 1% (noisy case) of the largest recovered coefficient in each gene equation (with the exception of the noiseless-case Oct4 equation, thresholded at 0.01% to show the successful recovery of weak edges). The algorithm performs almost perfectly in the noiseless case, except for a false positive repressor on Gata6 and two very weak activation edges missing. In the noisy case, the algorithm recovers all of the strong edges, but misses some of the weaker ones and returns a few small false positives at our chosen thresholding level. Overall, the method captures the major network structure even in the noisy case.

ered almost exactly:

$$\begin{aligned}
 \frac{d[O]}{dt} &= (0.001 + [A] + (0.005[O][S] + 0.025[O][S][N])) \\
 &\quad / (1 + [A] + (0.001[O] + 0.005[O][S] + 0.025[O][S][N]) \\
 &\quad \quad \quad + 10[O][C] + 10[Gc]) \\
 &\quad - 0.1[O], \\
 (9) \quad \frac{d[S]}{dt} &= \frac{0.001 + 0.005[O][S] + 0.025[O][S][N]}{1 + 0.005[O][S] + 0.025[O][S][N]} - 0.1[S], \\
 \frac{d[N]}{dt} &= \frac{0.1[O][S] + 0.1[O][S][N]}{1 + 0.1[O][S] + 0.1[O][S][N] + 10[O][G]} - 0.1[N], \\
 \frac{d[C]}{dt} &= \frac{2[C]}{1 + 2[C] + 5[O][C]} - 0.1[C], \\
 \frac{d[Gc]}{dt} &= \frac{0.001 + 0.1[C] + 0.1[G]}{1 + 0.1[C] + 0.1[G]} - 0.1[Gc], \\
 \frac{d[G]}{dt} &= \frac{0.1 + [O]}{1 + [O] + 0.03[N][Gc] + 15[N]} - 0.1[G].
 \end{aligned}$$

Next we add zero-mean Gaussian noise to each measurement, with standard deviation 1% of the measurement magnitude. We use the same steady-states as in the noiseless case, plus overexpression-knockdown of each pair of genes starting from ESC and DSC. Using a similar approach (detailed in section S3 of the supplement), we recover:

$$\begin{aligned}
 \frac{d[O]}{dt} &= \frac{[A]}{1 + [A] + 9.9[Gc] + 9.9[O][C]} - 0.1[O], \\
 \frac{d[S]}{dt} &= \frac{0.001[O][S] + 0.0005[S][N] + 0.025[O][S][N]}{1 + 0.001[O][S] + 0.0005[S][N] + 0.025[O][S][N]} - 0.1[S], \\
 (10) \quad \frac{d[N]}{dt} &= \frac{0.09[O][S][N]}{1 + 0.1[G][Gc] + 0.09[O][S][N] + 9.1[O][G]} - 0.1[N], \\
 \frac{d[C]}{dt} &= \frac{2[C]}{1 + 2[C] + 5[O][C]} - 0.1[C], \\
 \frac{d[Gc]}{dt} &= \frac{0.1[C] + 0.1[G]}{1 + 0.1[C] + 0.1[G]} - 0.1[Gc], \\
 \frac{d[G]}{dt} &= \frac{0.1 + 0.9[O]}{1 + 0.9[O] + 14.2[N]} - 0.1[G].
 \end{aligned}$$

In order to produce clean equations and network diagrams, we choose appropriate thresholds for each equation below which we zero the coefficients. (In practice,

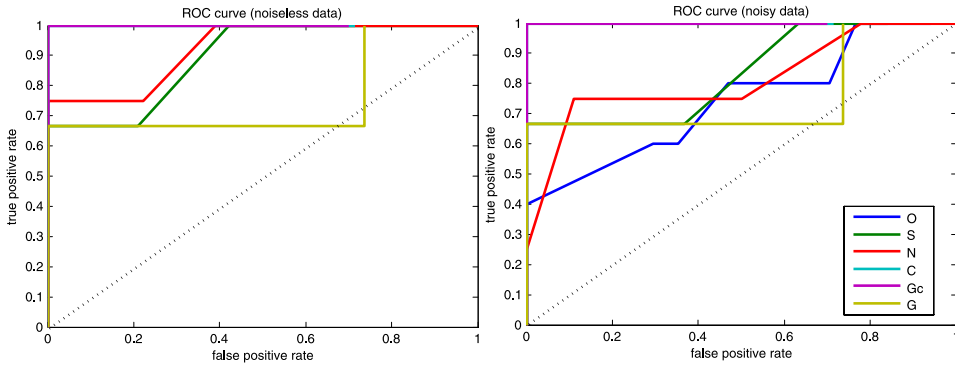


FIG. 5. ROC curves for recovered networks from noiseless (left) and noisy (right) data showing the trade-off between true positive rate (TPR) and false positive rate (FPR) for edge recovery. The ROC curves show the TPR and FPR that result from a range of coefficient threshold choices above which we consider an edge to have been recovered. For the equation $dx_i/dt = \dots$ and threshold t , TPR is defined as the proportion of true edges j with $c_{ij}^{\text{recovered}} > t$ and FPR as the proportion of false edges with $c_{ij}^{\text{recovered}} > t$. For equations with two possible forms, we compare the simple forms of the true and recovered equations. Each gene equation has a different ROC curve as indicated by the legend. The dotted black line is the expected ROC curve for the “random guessing” algorithm, while the (0, 1) point corresponds to a perfect algorithm (in fact, our algorithm performs perfectly for the Gcnf equation).

choosing thresholds is a judgment call based on the expected number of regulators, the noise level of the data and the level of detail appropriate for the application.) We set the thresholds at 0.1% (noiseless case) or 1% (noisy case) of the largest coefficient recovered for each equation. For example, the largest recovered coefficient in the $d[G]/dt$ equation is roughly 15 in either case, so we zero the coefficients that fall below 0.015 (noiseless case) or 0.15 (noisy case). The recovered systems of equations shown above reflect these choices. In the noiseless case, relaxing the threshold on the Oct4 equation to 0.01% leads to the recovery of more correct terms, listed in parentheses. For completeness, we also provide receiver operating characteristic (ROC) curves in Figure 5 to show the trade-off between true positives and false positives at other thresholds. The network diagrams in Figure 4(b), (c) include an edge if the corresponding coefficient is above the threshold, with weights reflecting the size of the coefficients. These diagrams show that the recovery is nearly perfect in the noiseless case: using the gentler threshold for the Oct4 equation, we recover all the true edges except for three very weak ones, and return just one small false positive repressor in the Gata6 equation. In the noisy case, we recover all the large coefficients correctly, although there are a few small false positives and we miss several of the weakest edges. Overall, the method is able to capture the major network structure.

Discussion. Our experiment on the synthetic ESC system demonstrates that our algorithm can be used to infer a complex dynamical systems model of gene regulation and that the method can tolerate low levels of noise. Term selection from among all possible single gene and gene-complex regulators (up to second-degree interactions, plus the third-degree interaction OSN) was successful. The inferred equations are easy to interpret in terms of gene networks, and the detailed quantitative information allows for prediction of future expression trajectories from any starting point.

The approach is also scalable. Since we have formulated our problem as a convex optimization problem [equation (4)], it can be solved efficiently even for large systems using prepackaged software. Furthermore, it is trivially parallelizable, since we need to solve a version of (4) to infer the differential equation coefficients b_{ij}, c_{ij} for each gene i . Parallelization is even more helpful for the cross-validation step, where we need to solve equation (4) for each gene and a sequence of choices sparsity parameter λ . We tested the scalability by running the algorithm with the parallelization discussed above on a simulated 100-gene system. The algorithm ran correctly in a reasonable time frame (a few hours) on a computing cluster.

The high resolution of our model is one of its most valuable features, but it means that accurate term selection may require much data, especially in the presence of noise. In our experiment, when we added 1% Gaussian noise, we needed extra data (knockdown/overexpression pairs) in order to accurately select terms. When we tried 5% noise, the algorithm consistently selected the large terms in five of the six equations, but we had to add even more data in order to correctly identify the major repressor in the Nanog equation. The Nanog equation is subtle in that Oct4 acts as both an activator in complexes with Sox2 and Nanog and a repressor in a complex with Gata6, so the algorithm tends to select different Gata6 complexes (or the Gata6 singleton) as the major repressor when the data is insufficient. In the 5% noise case, we needed additional data on the role of Gata6 (double-knockdowns and double-overexpression of pairs including Gata6 from ESC and DSC) in order to select Oct4-Gata6 as the major repressor of Nanog fairly consistently. As discussed earlier, another difficulty is the nonidentifiability that arises from accounting for self-regulation while restricting data to steady-states. Distinguishing between the two possible forms of nonidentifiable equations requires extra derivative data (which can be collected experimentally, although it is more difficult and time-consuming) and extra steps in the algorithm. The constraints on the convex optimization problem (4), which arise from thermodynamic considerations, are sufficient to prevent further nonidentifiability, but in certain cases, certain problems can suffer from near-nonidentifiability of other forms, which may contribute to the challenge of term-selection with noisy or limited data. We ensure accurate term selection by making sure we include enough diverse, high-quality steady-state measurements.

We should also note that our model does not account for the intrinsic noise in gene transcription and translation, although these processes are inherently stochastic, since TF and RNAP binding result from chance collisions between molecules

in the cell. However, the stochastic version of our rational-form transcription model is highly complex and there is currently no satisfactory method for its inference. Studying the deterministic evolution plus additive noise is standard practice for all but linear models of gene expression, and treatment of the deterministic model provides insight into the stochastic model. Here we focus on the additive noise case and leave the study of intrinsic noise for future investigation.

Conclusions. The model we use is based on the detailed thermodynamics of gene transcription, and quantitatively captures the full spectrum of regulatory phenomena in a detailed, physically interpretable, predictive manner. Since we can formulate the model fitting problem as a convex optimization problem, we can solve it efficiently and scalably using prepackaged software. ℓ_1 -regularization allows for term-selection while maintaining the problem convexity. The experiments required to collect the necessary steady-state gene expression data are straightforward to perform, as technologies for knockdowns and overexpression are well-established and measuring gene expression is relatively simple. The model accounts for activation and repression by single-protein TFs and synergistic complexes as well as self-regulation, and describes the magnitude of each type of regulation in quantitative detail. Furthermore, the model can be extended to account for environmental effects and auxiliary proteins involved in regulation, including enhancers and chromatin remodelers. The fitted model can predict the evolution of the system from any starting point. Given a set of steady-states gene expression measurements, our algorithm can be used to fit a model which not only predicts further steady-states of the system, but also fully describes the transitions between them. Finally, beside the study of gene regulation, our approach will be useful in many other application areas where it is necessary to infer a nonlinear dynamical system by suitable experimentation and statistical analysis.

APPENDIX: THERMODYNAMIC MODEL

In (1), the function $f_i(y)$ represents the probability that RNAP binds to the i th gene promoter. We claim that $f_i(y)$ has the form

$$f_i(y) \equiv P_{\text{bound}}^{(i)}(y) = \frac{\sum_j e^{-\beta \Delta \varepsilon_{ij}^{\text{RNAP}}} P e^{-\beta \Delta \varepsilon_{ij}} \prod_{k \in S_{ij}} y_k}{\sum_j (1 + e^{-\beta \Delta \varepsilon_{ij}^{\text{RNAP}}} P) e^{-\beta \Delta \varepsilon_{ij}} \prod_{k \in S_{ij}} y_k},$$

where $\Delta \varepsilon_{ij}$ is the binding energy of the j th complex to the promoter, $\Delta \varepsilon_{ij}^{\text{RNAP}}$ is the binding energy of RNAP to the j th promoter-bound complex, and P, x_j are the concentrations of RNAP and gene product j [Bintu et al. (2005a, 2005b)].

Any type of regulator (including no regulator at all) can be represented in this framework. For no regulator, we take $S_{ij} = \emptyset$ with the convention that $\prod_{k \in \emptyset} y_k = 1$, set $\Delta \varepsilon_{ij} = 0$, and take $\Delta \varepsilon_{ij}^{\text{RNAP}}$ as the base binding energy of RNAP to the

promoter. For a repressor, $\Delta\varepsilon_{ij} < 0$ and $\Delta\varepsilon_{ij}^{\text{RNAP}} > 0$; for an activator, $\Delta\varepsilon_{ij} < 0$ and $\Delta\varepsilon_{ij}^{\text{RNAP}} < 0$.

Setting

$$b_{ij} = e^{-\beta\Delta\varepsilon_{ij}^{\text{RNAP}}} P e^{-\beta\Delta\varepsilon_{ij}},$$

$$c_{ij} = (1 + e^{-\beta\Delta\varepsilon_{ij}^{\text{RNAP}}} P) e^{-\beta\Delta\varepsilon_{ij}},$$

we obtain the form given in Section 1:

$$f_i(y) = \frac{b_{ij} \prod_{k \in S_{ij}} y_k}{\sum_j c_{ij} \prod_{k \in S_{ij}} y_k}.$$

Constant terms in the numerator and denominator correspond to the no-regulator case. Letting c_{i0} denote the constant appearing in the denominator, our convention will be to divide all of the coefficients in the numerator and denominator by c_{i0} so that the constant 1 appears in the denominator.

Simplified derivation. The derivation we present here follows Bintu et al. and Garcia et al. [Bintu et al. (2005a, 2005b), Garcia et al. (2011)]. For simplicity, we will prove the following claim for the simplified case with one regulator y_1 (as well as the possibility of RNAP binding with no regulator):

$$p_{\text{bound}}^{(i)} = \frac{e^{-\beta\Delta\varepsilon_{i0}^{\text{RNAP}}} p + e^{-\beta\Delta\varepsilon_{i1}^{\text{RNAP}}} p e^{-\beta\Delta\varepsilon_{i1}} y_1}{(1 + e^{-\beta\Delta\varepsilon_{i0}^{\text{RNAP}}} p) + (1 + e^{-\beta\Delta\varepsilon_{i1}^{\text{RNAP}}} p) e^{-\beta\Delta\varepsilon_{i1}} y_1}.$$

We will use the following notation: $\varepsilon_{P,i1}^S$ is the energy of the state in which RNAP is specifically bound to the regulator-promoter complex, $\varepsilon_{P,i0}^S$ is the energy of the state in which RNAP is specifically bound to the promoter without the regulator, $\varepsilon_P^{\text{NS}}$ is the energy when RNAP is bound to a nonspecific binding site, ε_{i1}^S is the energy when y_1 is specifically bound to the promoter, and $\varepsilon_{i1}^{\text{NS}}$ is energy when y_1 is bound to a nonspecific binding site. Then

$$\Delta\varepsilon_{i0}^{\text{RNAP}} = \Delta\varepsilon_{P,i0} \equiv \varepsilon_{P,i0}^S - \varepsilon_P^{\text{NS}},$$

$$\Delta\varepsilon_{i1}^{\text{RNAP}} = \Delta\varepsilon_{P,i1} \equiv \varepsilon_{P,i1}^S - \varepsilon_P^{\text{NS}}, \quad \Delta\varepsilon_{i1} \equiv \varepsilon_{y_1}^S - \varepsilon_{y_1}^{\text{NS}}.$$

Suppose that we have j RNA polymerase molecules and k molecules of gene product 1 (the regulator). We model the genome as a “reservoir” with n nonspecific binding sites (to which either RNAP or regulator can bind). One of these sites is the promoter of gene i . Four different classes of configurations interest us:

1. empty promoter,
2. regulator bound to promoter,
3. regulator and RNAP bound to promoter,
4. RNAP only bound to promoter.

These correspond to the following partial partition functions, which represent the “unnormalized probabilities” of each configuration:

1. $Z(j, k)$,
2. $Z(j, k - 1)e^{-\beta\varepsilon_{i1}^S}$,
3. $Z(j - 1, k - 1)e^{-\beta\varepsilon_{i1}^S}e^{-\beta\varepsilon_{P,i1}^S}$,
4. $Z(j - 1, k)e^{-\beta\varepsilon_{P,i0}^S}$,

where $Z(j, k) = \frac{n!}{j!k!(n-j-k)!}e^{-\beta r\varepsilon_{i1}^{NS}}e^{-\beta\varepsilon_P^{NS}}$.

$Z(j, k)$ is equal to the total number of arrangements of RNAP and regulator on the nonspecific binding sites times the Boltzmann factor, which gives the relative probability $e^{-\beta\varepsilon}$ of a particular state in terms of its energy ε .

Since RNAP binds the promoter only in the third and fourth classes of configurations, the probability that RNAP binds the promoter is equal to the unnormalized probability of the third and fourth configurations divided by the “total probability” (the sum of the unnormalized probabilities of all classes of configurations). Hence,

$$\begin{aligned}
 p_{\text{bound}} &= (Z(j - 1, k)e^{-\beta\varepsilon_{P,i0}^S} + Z(j - 1, k - 1)e^{-\beta\varepsilon_{i1}^S}e^{-\beta\varepsilon_{P,i1}^S}) \\
 &\quad / (Z(j, k) + Z(j - 1, k)e^{-\beta\varepsilon_{P,i0}^S} \\
 &\quad + Z(j, k - 1)e^{-\beta\varepsilon_{i1}^S} + Z(j - 1, k - 1)e^{-\beta\varepsilon_{i1}^S}e^{-\beta\varepsilon_{P,i1}^S}) \\
 &\approx \left(\frac{n^{j-1}n^k}{(j-1)!k!}e^{-\beta k\varepsilon_{i1}^{NS}}e^{-\beta(j-1)\varepsilon_P^{NS}}e^{-\beta\varepsilon_{P,i0}^S} \right. \\
 &\quad \left. + \frac{n^{j-1}n^{k-1}}{(j-1)!(k-1)!}e^{-\beta(k-1)\varepsilon_{i1}^{NS}}e^{-\beta(j-1)\varepsilon_P^{NS}}e^{-\beta\varepsilon_{i1}^S}e^{-\beta\varepsilon_{P,i1}^S} \right) \\
 &\quad / \left(\frac{n^j n^k}{j!k!}e^{-\beta k\varepsilon_{i1}^{NS}}e^{-\beta j\varepsilon_P^{NS}} \right. \\
 &\quad \left. + \frac{n^{j-1}n^k}{(j-1)!k!}e^{-\beta k\varepsilon_{i1}^{NS}}e^{-\beta(j-1)\varepsilon_P^{NS}}e^{-\beta\varepsilon_{P,i0}^S} + \dots \right) \\
 &= \left(\frac{j}{n}e^{\beta\varepsilon_P^{NS}}e^{-\beta\varepsilon_{P,i0}^S} + \frac{j}{n}\frac{k}{n}e^{\beta\varepsilon_{i1}^{NS}}e^{\beta\varepsilon_P^{NS}}e^{-\beta\varepsilon_{i1}^S}e^{-\beta\varepsilon_{P,i1}^S} \right) \\
 &\quad / \left(1 + \frac{j}{n}e^{\beta\varepsilon_P^{NS}}e^{-\beta\varepsilon_{P,i0}^S} + \frac{k}{n}e^{\beta\varepsilon_{i1}^{NS}}e^{-\beta\varepsilon_{i1}^S} \right. \\
 &\quad \left. + \frac{j}{n}\frac{k}{n}e^{\beta\varepsilon_{i1}^{NS}}e^{\beta\varepsilon_P^{NS}}e^{-\beta\varepsilon_{i1}^S}e^{-\beta\varepsilon_{P,i1}^S} \right) \\
 &= \frac{(j/n)e^{-\beta\Delta\varepsilon_{P,i0}} + (j/n)(k/n)e^{-\beta\Delta\varepsilon_{i1}}e^{-\beta\Delta\varepsilon_{P,i1}}}{1 + (j/n)e^{-\beta\Delta\varepsilon_{P,i0}} + (k/n)e^{-\beta\Delta\varepsilon_{i1}} + (j/n)(k/n)e^{-\beta\Delta\varepsilon_{i1}}e^{-\beta\Delta\varepsilon_{P,i1}}}
 \end{aligned}$$

$$\begin{aligned}
&= \frac{(j/n)e^{-\beta\Delta\varepsilon_{P,i0}} + (j/n)(k/n)e^{-\beta\Delta\varepsilon_{i1}}e^{-\beta\Delta\varepsilon_{P,i1}}}{1 + (j/n)e^{-\beta\Delta\varepsilon_{P,i0}} + (k/n)e^{-\beta\Delta\varepsilon_{i1}}(1 + (j/n)e^{-\beta\Delta\varepsilon_{P,i1}})} \\
&= \frac{pe^{-\beta\Delta\varepsilon_{i0}^{\text{RNAP}}} + py_1e^{-\beta\Delta\varepsilon_{i1}}e^{-\beta\Delta\varepsilon_{i1}^{\text{RNAP}}}}{1 + pe^{-\beta\Delta\varepsilon_{i0}^{\text{RNAP}}} + y_1e^{-\beta\Delta\varepsilon_{i1}}(1 + pe^{-\beta\Delta\varepsilon_{i1}^{\text{RNAP}}})},
\end{aligned}$$

where in the second line we used the approximation $\frac{n!}{j!k!(n-j-k)!} \approx \frac{n^j n^k}{j!k!}$ which holds for $j, k \ll n$, in the third we divided by $\frac{n^j n^k}{j!k!} e^{-\beta k \varepsilon_{i1}^{\text{NS}}} e^{-\beta \varepsilon_P^{\text{NS}}}$, in the fourth we used the identities $\Delta\varepsilon_{P,i0} = \varepsilon_{P,i0}^S - \varepsilon_P^{\text{NS}}$, $\Delta\varepsilon_{P,i1} = \varepsilon_{P,i1}^S - \varepsilon_P^{\text{NS}}$, $\Delta\varepsilon_{i1} \equiv \varepsilon_{i1}^S - \varepsilon_{i1}^{\text{NS}}$, and in the last we substituted in the definitions $\frac{j}{n} = p$, $\frac{k}{n} = y_1$, $\Delta\varepsilon_{i0}^{\text{RNAP}} = \Delta\varepsilon_{P,i0}$, $\Delta\varepsilon_{i1}^{\text{RNAP}} = \Delta\varepsilon_{P,i1}$.

Acknowledgments. Many thanks to Xi Chen for helpful discussions.

SUPPLEMENTARY MATERIAL

Nonidentifiability, tie-breaking and synthetic network study details (DOI: [10.1214/13-AOAS645SUPP](https://doi.org/10.1214/13-AOAS645SUPP); .pdf). We discuss nonidentifiability and tie-breaking in Sections S1 and S2 by proving the equivalence of two different equation forms at steady-state and describing methods for determining the true form of an ambiguous equation. In Section S3 we provide the details of our study of a simulated six-gene network in mouse ESC, including parameter selection, tie-breaking and thresholding.

REFERENCES

- ACKERS, G. K., JOHNSON, A. D. and SHEA, M. A. (1982). Quantitative model for gene regulation by lambda phage repressor. *Proc. Natl. Acad. Sci. USA* **79** 1129–1133.
- ALBERTS, B., JOHNSON, A., LEWIS, J., RAFF, M., ROBERTS, K. and WALTER, P. (2007). *Molecular Biology of the Cell*, 5th ed. Garland, New York, NY.
- ALON, U. (2007). Network motifs: Theory and experimental approaches. *Nat. Rev. Genet.* **8** 450–461.
- AVERY, L. and WASSERMAN, S. (1992). Ordering gene function: The interpretation of epistasis in regulatory hierarchies. *Trends Genet.* **8** 312–316.
- BANSAL, M., BELCASTRO, V., AMBESI-IMPIOMBATO, A. and DI BERNARDO, D. (2007). How to infer gene networks from expression profiles. *Mol. Syst. Biol.* **3** 78.
- BAR-JOSEPH, Z., GERBER, G. K., LEE, T. I., RINALDI, N. J., YOO, J. Y., ROBERT, F., GORDON, D. B., FRAENKEL, E., JAAKKOLA, T. S., YOUNG, R. A. and GIFFORD, D. K. (2003). Computational discovery of gene modules and regulatory networks. *Nat. Biotechnol.* **21** 1337–1342.
- BINTU, L., BUCHLER, N. E., GARCIA, H. G., GERLAND, U., HWA, T., KONDEV, J., KUHLMAN, T. and PHILLIPS, R. (2005a). Transcriptional regulation by the numbers: Applications. *Curr. Opin. Genet. Dev.* **15** 125–135.
- BINTU, L., BUCHLER, N. E., GARCIA, H. G., GERLAND, U., HWA, T., KONDEV, J. and PHILLIPS, R. (2005b). Transcriptional regulation by the numbers: Models. *Curr. Opin. Genet. Dev.* **15** 116–124.

- CHICKARMANE, V. and PETERSON, C. (2008). A computational model for understanding stem cell, trophoctoderm and endoderm lineage determination. *PLoS ONE* **3** e3478.
- CHOI, B. (2012). Learning networks in biological systems. Ph.D. thesis, Dept. Applied Physics, Stanford Univ., Stanford, CA (thesis supervisor: W. H. Wong).
- CRICK, F. (1970). Central dogma of molecular biology. *Nature* **227** 561–563.
- DE SMET, R. and MARCHAL, K. (2010). Advantages and limitations of current network inference methods. *Nat. Rev. Microbiol.* **8** 717–729.
- DEHMER, M., EMMERT-STREIB, F., GRABER, A. and SALVADOR, A. (2011). *Applied Statistics for Network Biology*. Wiley, Weinheim.
- DERISI, J. L., IYER, V. R. and BROWN, P. O. (1997). Exploring the metabolic and genetic control of gene expression on a genomic scale. *Science* **278** 680–686.
- EISEN, M. B., SPELLMAN, P. T., BROWN, P. O. and BOTSTEIN, D. (1998). Cluster analysis and display of genome-wide expression patterns. *Proc. Natl. Acad. Sci. USA* **95** 14863–14868.
- FAITH, J. J., HAYETE, B., THADEN, J. T., MOGNO, I., WIERZBOWSKI, J., COTTAREL, G., KASIF, S., COLLINS, J. J. and GARDNER, T. S. (2007). Large-scale mapping and validation of Escherichia coli transcriptional regulation from a compendium of expression profiles. *PLoS Biol.* **5** e8.
- FOYCEL, K., CHOI, B., JUN, S., LEONG, D. E., LEE, A., WONG, C. C., ZUO, E., ECKART, M., REIJO PERA, R. A., WONG, W. H. and YAO, M. W. (2008). A novel and critical role for Oct4 as a regulator of the maternal-embryonic transition. *PLoS One* **3** e4109.
- FRIEDMAN, N. (2004). Inferring cellular networks using probabilistic graphical models. *Science* **303** 799–805.
- GARCIA, H. G., KONDEV, J., ORME, N., THERIOT, J. A. and PHILLIPS, R. (2011). Thermodynamics of biological processes. *Meth. Enzymol.* **492** 27–59.
- GARDNER, T. S., DI BERNARDO, D., LORENZ, D. and COLLINS, J. J. (2003). Inferring genetic networks and identifying compound mode of action via expression profiling. *Science* **301** 102–105.
- HARTWELL, L., HOOD, L., GOLDBERG, M., REYNOLDS, A. and SILVER, L. (2010). *Genetics: From Genes to Genomes*, 4th ed. McGraw-Hill, New York.
- HOLSTEGE, F. C., JENNINGS, E. G., WYRICK, J. J., LEE, T. I., HENGARTNER, C. J., GREEN, M. R., GOLUB, T. R., LANDER, E. S. and YOUNG, R. A. (1998). Dissecting the regulatory circuitry of a eukaryotic genome. *Cell* **95** 717–728.
- HU, Z., KILLION, P. J. and IYER, V. R. (2007). Genetic reconstruction of a functional transcriptional regulatory network. *Nat. Genet.* **39** 683–687.
- HUANG, S., EICHLER, G., BAR-YAM, Y. and INGBER, D. E. (2005). Cell fates as high-dimensional attractor states of a complex gene regulatory network. *Phys. Rev. Lett.* **94** 128701.
- HUGHES, T. R., MARTON, M. J., JONES, A. R., ROBERTS, C. J., STOUGHTON, R., ARMOUR, C. D., BENNETT, H. A., COFFEY, E., DAI, H., HE, Y. D., KIDD, M. J., KING, A. M., MEYER, M. R., SLADE, D., LUM, P. Y., STEPANIANS, S. B., SHOEMAKER, D. D., GACHOTTE, D., CHAKRABURTTY, K., SIMON, J., BARD, M. and FRIEND, S. H. (2000). Functional discovery via a compendium of expression profiles. *Cell* **102** 109–126.
- JACOB, F. and MONOD, J. (1961). Genetic regulatory mechanisms in the synthesis of proteins. *J. Mol. Biol.* **3** 318–356.
- LEE, T. I., RINALDI, N. J., ROBERT, F., ODOM, D. T., BAR-JOSEPH, Z., GERBER, G. K., HANNETT, N. M., HARBISON, C. T., THOMPSON, C. M., SIMON, I., ZEITLINGER, J., JENNINGS, E. G., MURRAY, H. L., GORDON, D. B., REN, B., WYRICK, J. J., TAGNE, J. B., VOLKERT, T. L., FRAENKEL, E., GIFFORD, D. K. and YOUNG, R. A. (2002). Transcriptional regulatory networks in Saccharomyces cerevisiae. *Science* **298** 799–804.
- LENGNER, C. J., CAMARGO, F. D., HOCHEDLINGER, K., WELSTEAD, G. G., ZAIDI, S., GOKHALE, S., SCHOLER, H. R., TOMILIN, A. and JAENISCH, R. (2011). Oct4 expression is not required for mouse somatic stem cell self-renewal. *Cell Stem Cell* **1** 403–415.

- MARBACH, D., PRILL, R. J., SCHAFFTER, T., MATTIUSI, C., FLOREANO, D. and STOLOVITZKY, G. (2010). Revealing strengths and weaknesses of methods for gene network inference. *Proc. Natl. Acad. Sci. USA* **107** 6286–6291.
- MEISTER, A., LI, Y. H., CHOI, B. and WONG, W. H. (2013). Supplement to “Learning a nonlinear dynamical system model of gene regulation: A perturbed steady-state approach.” DOI:10.1214/13-AOAS645SUPP.
- MORTAZAVI, A., WILLIAMS, B. A., MCCUE, K., SCHAEFFER, L. and WOLD, B. (2008). Mapping and quantifying mammalian transcriptomes by RNA-Seq. *Nat. Methods* **5** 621–628.
- PALSSON, B. (2011). *Systems Biology: Simulation of Dynamic Network States*. Cambridge Univ. Press, Cambridge.
- PINNA, A., SORANZO, N. and DE LA FUENTE, A. (2010). From knockouts to networks: Establishing direct cause-effect relationships through graph analysis. *PLoS ONE* **5** e12912.
- REN, B., ROBERT, F., WYRICK, J. J., APARICIO, O., JENNINGS, E. G., SIMON, I., ZEITLINGER, J., SCHREIBER, J., HANNETT, N., KANIN, E., VOLKERT, T. L., WILSON, C. J., BELL, S. P. and YOUNG, R. A. (2000). Genome-wide location and function of DNA binding proteins. *Science* **290** 2306–2309.
- ROBERTSON, G., HIRST, M., BAINBRIDGE, M., BILENKY, M., ZHAO, Y., ZENG, T., EUSKIRCHEN, G., BERNIER, B., VARHOL, R., DELANEY, A., THIESSEN, N., GRIFFITH, O. L., HE, A., MARRA, M., SNYDER, M. and JONES, S. (2007). Genome-wide profiles of STAT1 DNA association using chromatin immunoprecipitation and massively parallel sequencing. *Nat. Methods* **4** 651–657.
- RODRIGUEZ, R. T., VELKEY, J. M., LUTZKO, C., SEERKE, R., KOHN, D. B., O’SHEA, K. S. and FIRPO, M. T. (2007). Manipulation of OCT4 levels in human embryonic stem cells results in induction of differential cell types. *Exp. Biol. Med. (Maywood)* **232** 1368–1380.
- ROSENFELD, S. (2011). Mathematical descriptions of biochemical networks: Stability, stochasticity, evolution. *Prog. Biophys. Mol. Biol.* **106** 400–409.
- SCHAFFTER, T., MARBACH, D. and FLOREANO, D. (2011). GeneNetWeaver: In silico benchmark generation and performance profiling of network inference methods. *Bioinformatics* **27** 2263–2270.
- SEGAL, E., SHAPIRA, M., REGEV, A., PE’ER, D., BOTSTEIN, D., KOLLER, D. and FRIEDMAN, N. (2003). Module networks: Identifying regulatory modules and their condition-specific regulators from gene expression data. *Nat. Genet.* **34** 166–176.
- SHEA, M. A. and ACKERS, G. K. (1985). The OR control system of bacteriophage lambda. A physical-chemical model for gene regulation. *J. Mol. Biol.* **181** 211–230.
- TEGNER, J., YEUNG, M. K. S., HASTY, J. and COLLINS, J. J. (2003). Reverse engineering gene networks: Integrating genetic perturbations with dynamical modeling. *Proc. Natl. Acad. Sci. USA* **100** 5944–5949.
- TIBSHIRANI, R. (1996). Regression shrinkage and selection via the lasso. *J. R. Stat. Soc. Ser. B Stat. Methodol.* **58** 267–288. MR1379242
- TYSON, J. J., CHEN, K. C. and NOVAK, B. (2003). Sniffers, buzzers, toggles and blinkers: Dynamics of regulatory and signaling pathways in the cell. *Curr. Opin. Cell Biol.* **15** 221–231.
- VON HIPPEL, P. H., REVZIN, A., GROSS, C. A. and WANG, A. C. (1974). Non-specific DNA binding of genome regulating proteins as a biological control mechanism: I. The lac operon: Equilibrium aspects. *Proc. Natl. Acad. Sci. USA* **71** 4808–4812.
- WINZELER, E. A. (1999). Functional characterization of the *S. cerevisiae* genome by gene deletion and parallel analysis. *Science* **285** 901–906.
- YIP, K. Y., ALEXANDER, R. P., YAN, K.-K. and GERSTEIN, M. (2010). Improved reconstruction of in silico gene regulatory networks by integrating knockout and perturbation data. *PLoS ONE* **5** e8121.

- ZAFARANA, G., AVERY, S. R., AVERY, K., MOORE, H. D. and ANDREWS, P. W. (2009). Specific knockdown of OCT4 in human embryonic stem cells by inducible short hairpin RNA interference. *Stem Cells* **27** 776–782.
- ZHOU, Q., CHIPPERFIELD, H., MELTON, D. A. and WONG, W. H. (2007). A gene regulatory network in mouse embryonic stem cells. *Proc. Natl. Acad. Sci. USA* **408** 16438–16443.

DEPARTMENT OF STATISTICS
STANFORD UNIVERSITY
SEQUOIA HALL
390 SERRA MALL
USA
E-MAIL: arwenb@stanford.edu
ywli@stanford.edu
bkchoi@stanford.edu
whwong@stanford.edu